2010

High magnetization aqueous ferrofluid: A simple one-pot synthesis

Kyler J. Carroll
Virginia Commonwealth University

Michael D. Schultz
Virginia Commonwealth University

Panos P. Fatouros
Virginia Commonwealth University

Everett E. Carpenter
Virginia Commonwealth University, ecarpenter2@vcu.edu

Carroll, K. J., Schultz, M. D., & Fatouros, P. P., et al. High magnetization aqueous ferrofluid: A simple one-pot synthesis. Journal of Applied Physics, 107, 09B304 (2010).

High magnetization aqueous ferrofluid: A simple one-pot synthesis

Kyler J. Carroll,[1] Michael D. Shultz,[2] Panos P. Fatouros,[2] and Everett E. Carpenter[1,a)]
[1]*Department of Chemistry, Virginia Commonwealth University, Richmond, Virginia 23284, USA*
[2]*Department of Radiology, Virginia Commonwealth University, Richmond, Virginia 23284, USA*

(Presented 22 January 2010; received 30 October 2009; accepted 2 December 2009; published online 20 April 2010)

A one-step polyol method was utilized to prepare a stable aqueous iron/iron oxide ferrofluid. The dried powders were characterized by x-ray diffraction, electron microscopy, x-ray absorption spectroscopy, and vibrating sample magnetometry for the determination of phase, morphology, and magnetic properties. To show its potential for imaging applications, the ferrofluid was also investigated as a magnetic resonance imaging contrast agent. © *2010 American Institute of Physics*. [doi:10.1063/1.3357342]

Stable colloidal suspensions of magnetic nanoparticles have many appealing qualities that have attracted them to areas of industry, biomedical engineering, physics, and chemistry. Many ferrofluids are used commercially as heat transfer fluids for dampeners in loud speakers, in electronic devices as a form of liquid seals for drive shafts in hard disks, and in medicine as contrast agents for magnetic resonance imaging (MRI) due to their T_1 and greater T_2 enhancement.[1–4] There are two main types of stabilizers for dispersing magnetic nanoparticles such as: surfactant/polymer stabilized nanoparticles and ionically stabilized nanoparticles. These stabilizers allow for the formation of colloidal metal and metal oxide nanoparticles by various types of chemical and physical interactions. For polar solvents, tetramethylammonium hydroxide is commonly used as an ionic stabilizer: the hydroxyl group forms at the nanoparticles surface, providing a negatively charged surface layer. The positively charged tetramethylammonium cation $[N(CH_3)_4^+]$ forms a diffuse shell in which neighboring particles will encounter electrostatic repulsion.[5–15] For nonpolar solvent based ferrofluids, surfactants, or polymers that attach to nanoparticles, such as oleic acid, impose steric effects on the neighboring nanoparticles. The hydrocarbon has a polar head that has an affinity for the nanoparticle; the tail of the surfactant prevents the agglomeration of neighboring nanoparticles.[16] In each case, there are stringent rules which must be met in order to achieve effective stabilization. These rules affecting colloidal stability include parameters such as an optimum size range of the nanoparticles, viscosity of the carrier liquid, length of the surfactant, temperature, and magnetic field strength. Various techniques have been shown to produce magnetic nanoparticles such as: wet grinding, coprecipitation, microemulsion, and aqueous reduction in metal salts.[17–23] After the synthesis of the nanoparticles, additional steps are typically required to coat them with the appropriate stabilizer. In most cases, where the goal is an aqueous ferrofluid, the resulting nanoparticle is strictly an iron oxide. This work shows enhanced magnetic properties by forming aqueous stabilized metal/oxide core/shell nanoparticles. The oxide shell forms a passivation layer preventing further oxidation.[24]

This work presents an alternative method that provides an easier synthetic route and allows for the formation of metal/oxide composite nanoparticles. A modified polyol process is implemented, which allows for more controllable particle morphology along with an overall easier synthetic route. The use of a modified polyol process enabled the liquid polyol to act not only as a solvent but as a mild reducing agent. When coupled with a base, the polyol serves as the perfect medium for reduction in metal salt precursors, while also forming a stabilizing layer on the nanoparticle surface.[25–29] This ferrofluid was also investigated *in vitro* by magnetic resonance relaxivity measurements and *in vivo* for its application in MRI.

The synthesis of Fe/FeO_x nanoparticles was carried out under ambient conditions using a modified polyol method. First, two separate solutions were prepared, solution 1 and solution 2. Solution 1 contained 0.25 M iron(II) chloride tetrahydrate and 1,2 propanediol in a 500-ml round bottom flask and was heated to refluxing conditions for 30 min. Solution 2 containing 5.2 M NaOH and 1,2 propanediol was heated simultaneously at 100 °C with magnetic stirring. Hot solution 2 was subsequently added to solution 1 and heating was continued to refluxing conditions for one hour. The solution underwent a color change from dark orange, gray, and then finally jet black 20 min post addition. After 1 h the solution was allowed to cool to room temperature and then quenched by the addition of methanol. Throughout the reaction the particles did not seem to stick to the magnetic stirrer. The particles were washed with methanol several times and magnetically separated using a rare earth magnet. To prepare an aqueous ferrofluid, the particles were added to a vial with deionized water and sonicated to help the dispersion. The particles are stable in the aqueous media for over one year without visual degradation.

The nanoparticle morphology was confirmed by transmission electron microscopy (TEM) (Fig. 1), which revealed relative size uniformity with an average diameter of 15 (±2.5) nm; the sizes are consistent with dynamic light scattering (DLS) results. X-ray powder diffraction (Fig. 2) shows a mixed phase system with a face centered cubic magnetite

a)Author to whom correspondence should be addressed. Electronic mail: ecarpenter2@vcu.edu.

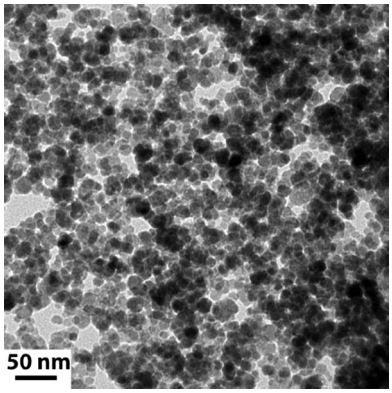

FIG. 1. TEM image of magnetite/α-Fe particles prepared by the polyol process in 1,2 propanediol. The TEM shows that the particles size distribution is relatively monodispersed.

and a body centered cubic iron. A linear combination fit to x-ray absorption near edge structure (XANES) data determined a composition of 20% metal and 80% oxide, which was also corroborated by Rietveld refinement on the x-ray diffraction (XRD) pattern yielding the same 20/80 ratio. Figure 3 shows the XANES spectra for the ferrofluid material, metallic iron foil and an iron oxide standard. Room temperature vibrating sample magnetometry revealed a saturation magnetization of 100 emu/g (Fig. 4). The saturation magnetization (M_s) was obtained from a magnetization versus 1/H plot and extrapolating to the point where 1/H is equal to zero. The values for bulk Fe and Fe_3O_4 are 220 emu/g and 80–120 emu/g, respectively. This value in magnetization for nanoparticles containing both iron and iron oxide is expected for the percentages of each component in this mixed phase system.

The nanoparticles also have a surfactant-type coating which will affect the magnetic characteristics of the nanoparticles, as well as act as the colloidal stabilizing agent. Thermal analysis of the dried particles reveals a 20% weight drop that correlates with an organic decomposition at 195 °C. The progressive heating of sodium hydroxide in the polyol not only reduces the Fe^{2+} to produce the nanoparticles but also forms a solution that plays an important role in the overall reaction dynamics. It is hypothesized that a sodium glycolate-type structure or 1,2 propanediol is adsorbed onto the surface of the particles allowing for *in situ* water stabilization. Further surface characterization will be needed to distinguish between the two possibilities. It is this structure

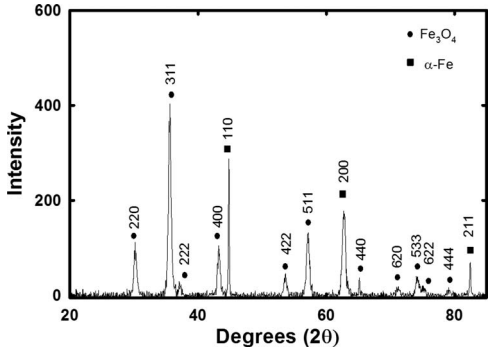

FIG. 2. XRD pattern showing a two-phase system of iron oxide and α-iron.

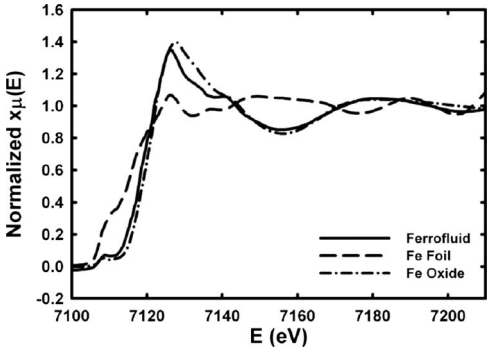

FIG. 3. XANES spectra for the ferrofluid material, and iron foil and iron oxide standards.

formed around the nanoparticle that gives both the colloidal stability and aids in the resistance to oxidation of the iron metal.

The MRI/spectroscopic experiments were performed on a 2.4 T/40 cm bore MR system (Biospec/Bruker). Spectroscopic T_1 and T_2 ^{1}H relaxation measurements of the aqueous ferrofluid were conducted using an inversion recovery sequence with eight inversion times and repetition times (TR) at least five times the expected T_1 value. For the T_2 measurements, a multispin-echo CPMG sequence was employed with several echo times and TR values at least five times the expected T_1. The relaxation times were computed from least-squares fitting of the exponentially varying signals using analysis routines available at the MR system. Relaxivities were extracted from graphs of relaxation rates ($1/T_1$ and $1/T_2$) versus concentration. The r_1 and r_2 relaxivities were found to be 8.6 and 382 s^{-1} mM^{-1}. These values should be compared to those reported for the commercial contrast agent Feridex, which are 12.3 and 191 s^{-1} mM^{-1}.[30]

The *in vivo* investigation was performed by intratumoral infusion of the aqueous ferrofluid via convection enhanced delivery[31–33] into a tumor bearing rat, 13 days post T9 tumor cell implantation. The aqueous ferrofluid was infused at *p*H 7.5, an iron concentration of 0.34 mM, and a rate of 0.2 μl/min for a total volume of 18 μL infused. The T_2-weighted images in Fig. 5 were acquired during the infusion and up to six days post. The dark contrast due to the ferrofluid is clearly seen in the center of the tumor during the infusion. Then 6 days post infusion, some of the ferrofluid

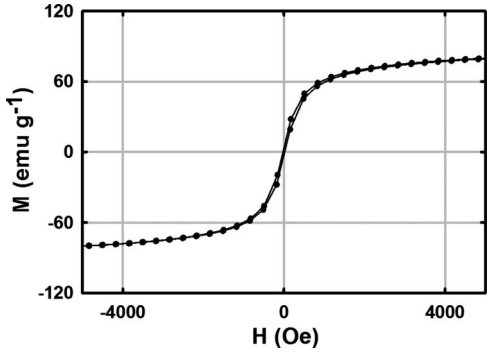

FIG. 4. Room temperature vibrating-sample magnetometer data plotted as magnetization (electromagnetic unit per gram) vs applied field (oersted).

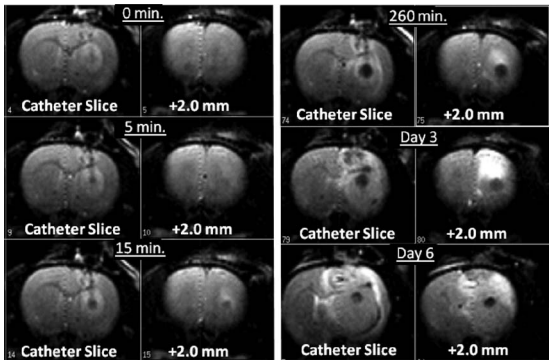

FIG. 5. T_2W images of a tumor-bearing rat infused with aqueous ferrofluid (0.34 mM iron concentration, 18 μl) at different time points. The infusate appears dark within the implanted T9 tumor (right side of the tumor). Note that at six-days post infusion, some of the iron/iron oxide particles have migrated in the tumor periphery (dark ring).

has pushed to the periphery, thereby more clearly defining the edge of the tumor.

In conclusion, an aqueous ferrofluid containing monodisperse Fe/FeO_x nanoparticles were produced using a modified one-pot polyol process. Controlling the reduction in the iron cations, along with the *in situ* stabilization results in particles with an enhanced magnetic moment over solely iron oxide based ferrofluids due to the incorporation of metallic iron and iron oxide phases in the nanoparticles. These ferrofluids have many promising aspects in biological applications and if linked with a biomolecule, could serve as promising magnetic carriers/labels for efficient bioseparation, drug delivery, and diagnostic applications.

ACKNOWLEDGMENTS

Microscopy was performed at the VCU-Dept. of Neurobiology & Anatomy Microscopy Facility, supported, in part, with funding from NIH-NINDS Center core grant (Grant No. 5P30NS047463).

[1]R. K. Bhatt, Ind. J. Eng. Mater. Sci. **5**, 477 (1998).
[2]S. Odenbach, *Ferrofluids* (Springer-Verlag, Bremen, Germany, 2002).
[3]S. Odenbach, *Magnetoviscous Effects in Ferrofluids* (Springer-Verlag, New York, 2002).
[4]M. D. Shultz, S. Calvin, P. P. Fatouros, S. A. Morrison, and E. E. Carpenter, J. Magn. Magn. Mater. **311**, 464 (2007).
[5]V. Badescu and R. Badescu, J. Optoelectron. Adv. Mater. **9**, 949 (2007).
[6]A. A. Bozhko, G. F. Putin, T. Tynjaelae, and P. Sarkomaa, J. Magn. Magn. Mater. **316**, 433 (2007).
[7]F. Döbrich, A. Michels, and R. Birringer, J. Magn. Magn. Mater. **316**, e779 (2007).
[8]J. P. Embs, C. Wagner, K. Knorr, and M. Lucke, EPL **78**, 44003 (2007).
[9]A. O. Ivanov, S. S. Kantorovich, E. N. Reznikov, C. Holm, A. F. Pshenichnikov, A. V. Lebedev, A. Chremos, and P. J. Camp, Phys. Rev. E **75**, 061405 (2007).
[10]V. Kuncser, G. Schinteie, B. Sahoo, W. Keune, D. Bica, L. Vekas, and G. Filoti, J. Phys.: Condens. Matter **19**, 016205 (2007).
[11]F. Larachi and D. Desvigne, China Particuol. **5**, 50 (2007).
[12]C.-F. Lee, Y.-H. Chou, and W.-Y. Chiu, J. Polym. Sci., Part A: Polym. Chem. **45**, 3062 (2007).
[13]M. Racuciu, D. E. Creanga, N. Apetroaie, and V. Badescu, J. Optoelectron. Adv. Mater. **9**, 1633 (2007).
[14]V. Salgueiriño-Maceira, L. M. Liz-Marzan, and M. Farle, Langmuir **20**, 6946 (2004).
[15]J. D. V. M. Schnorr, S. D. V. M. Wagner, C. D. V. M. Abramjuk, I. D. V. M. Wojner, T. P. Schink, T. J. M. D. Kroencke, E. M. D. Schellenberger, B. M. D. Hamm, H. P. Pilgrimm, and M. M. D. Taupitz, Invest. Radiol. **39**, 546 (2004).
[16]R. L. Carlin, *Magnetochemistry* (Springer-Verlag, New York, 1985).
[17]S. Papell, U.S. Patent No. 3215572 (1965).
[18]R. Massart, E. Dubois, V. Cabuil, and E. Hasmonay, J. Magn. Magn. Mater. **149**, 1 (1995).
[19]*Structure and Reactivity in Reverse Micelles*, edited by M. Pileni (Elsevier, Amsterdam, 1989).
[20]M. Pileni, T. Zemb, and C. Petit, Chem. Phys. Lett. **118**, 414 (1985).
[21]S. Harada and M. Ugaji, IEEE Trans. Magn. **8**, 468 (1972).
[22]G. Akashi, U.S. Patent No. 3607218 (1969).
[23]M. D. Shultz, W. Braxton, C. Taylor, and E. E. Carpenter, J. Appl. Phys. **105**, 07A522 (2009).
[24]E. E. Carpenter, S. Calvin, R. M. Stroud, and V. G. Harris, Chem. Mater. **15**, 3245 (2003).
[25]F. Fievet, F. Fievetvincent, J. P. Lagier, B. Dumont, and M. Figlarz, J. Mater. Chem. **3**, 627 (1993).
[26]F. Fievet, J. P. Lagier, B. Blin, B. Beaudoin, and M. Figlarz, Solid State Ionics **32–33**, 198 (1989).
[27]B. Blin, F. Fievet, D. Beaupere, and M. Figlarz, New J. Chem. **13**, 67 (1989).
[28]B. Blin, F. Fievet, J. P. Lagier, B. Beaudoin, and M. Figlarz, Journal De Chimie Physique Et De Physico-Chimie Biologique **84**, R15 (1987).
[29]F. Fievet, Surfactant Sci. Ser. **92**, 460 (2000).
[30]K. C. Briley-Saebo, V. Mani, F. Hyafil, J. C. Cornily, and Z. A. Fayad, Magn. Reson. Med. **59**, 721 (2008).
[31]W. C. Broaddus, S. S. Prabhu, G. T. Gillies, J. Neal, W. S. Conrad, Z. J. Chen, H. Fillmore, and H. F. Young, J. Neurosurg. **88**, 734 (1998).
[32]Z. J. Chen, G. T. Gillies, W. C. Broaddus, S. S. Prabhu, H. Fillmore, R. M. Mitchell, F. D. Corwin, and P. P. Fatouros, J. Neurosurg. **101**, 314 (2004).
[33]S. S. Prabhu, W. C. Broaddus, G. T. Gillies, W. G. Loudon, Z. J. Chen, and B. Smith, Surg. Neurol. **50**, 367 (1998).